ELSEVIER

Materials Chemistry and Physics 41 (1995) 104–109

MATERIALS CHEMISTRY AND PHYSICS

Characteristic analysis of ZnO varistors made with spherical precipitation powders

Shr-Nan Bai, Jen-Shame Shieh, Tseung-Yuen Tseng

Department of Electronics Engineering and Institute of Electronics, National Chiao-Tung University, Hsinchu, Taiwan, ROC

Received 19 October 1994; revised 15 March 1995; accepted 15 March 1995

Abstract

Small, uniform and spherical ZnO powders for the fabrication of ZnO varistors were obtained by an aqueous precipitation method. The varistor samples made from the ZnO powders using butylamine and urea as precipitant show excellent surge response characteristics. However, the varistor samples made by the ZnO–butylamine powders gave better electrical properties, including higher nonohmic property and lower leakage current, than those made by the ZnO–urea powders, because the ZnO powders precipitated by butylamine had smaller and more homogeneous size than those precipitated by urea.

Keywords: ZnO powder; Aqueous precipitation; Varistor; Electrical properties; Homogeneity

1. Introduction

ZnO varistors are highly nonohmic ceramic devices which are mainly composed of ZnO with minor additives of other metal oxides such as Bi_2O_3, CoO, MnO, Sb_2O_3 and Cr_2O_3 [1]. They are produced by a sintering process, which gives rise to a structure comprised of highly conductive ZnO grains surrounded by electrically insulating grain-boundary regions [2–5]. The microstructure of the ZnO varistors is therefore characterized by the multi-connection of individual nonohmic elements within the sintered body in series and parallel [6,7], which is similar to the microstructure of the SiC varistors. Such microstructure results in a greater energy-handling capability. Moreover, the nonohmic elements of the ZnO varistors have highly nonohmic electrical properties similar to those of Si Zener diodes [8]. As a result, the ZnO varistors can be considered to have both the advantages of SiC varistors and Si Zener diodes. Actually, it is because of their better withstanding-surge capability and nonohmic current–voltage electrical properties than other types of varistor devices [9] that the ZnO varistors are widely used in protecting power and signal level electrical circuits against dangerous voltage surges.

As is well known, the energy-handling capability is one of the most important requirements attendant on the application of the varistors for transient surge suppression. Nevertheless, the capability of the ZnO varistors is dependent not only on the composition and processing procedure, but also on the uniformity of the sintered body of the devices. A homogeneous sintered microstructure is required to control the thermal expansion and the consequent mechanical stresses arising from variation in resistance [10,11]; otherwise, the inhomogeneity of the sintered microstructure will make ZnO varistors fail by puncturing, which is caused by local melting, when the ZnO varistors are subjected to high energy pulses [12]. Amiji et al. [10] evaluated the homogeneity of the ZnO varistors by means of an IR radiation thermometer and found that thermal distribution was extremely consistent with the resistance distribution. In other words, when a current pulse was applied to the ZnO varistors, a large current flowed through the region with low resistance, while little current flowed through the region with high resistance. The region where a large current passed was consequently more likely to deteriorate.

From the above observations, a green pellet consisting of uniformly packed powders with a narrow size distribution is needed to achieve a homogeneous sintered microstructure. In order to get such uniformly packed powders with a narrow size distribution, it is suggested to make use of monosize, monodisperse, spherical powders [13–18], as these fine grain-size starting powders can be prepared by the method of aqueous precipitation.

Therefore, in our study we prepared ZnO powders with two different kinds of precipitant, urea and butylamine, and tried to produce ZnO particles as monosize and spherical as possible. With the same controlled condition of precipitation

SSDI 0254-0584(95)01540-B

from the solutions, we compared the properties of the ZnO varistors made from the powders using urea as precipitant and those using butylamine as precipitant.

2. Experimental procedure

2.1. Preparation of ZnO powders and varistor samples

The materials used in our study included reagent-grade methanol (MeOH; CH_3OH), triethanolamine (TEA; $C_6H_{15}NO_3$), zinc nitrate hexahydrate ($Zn(NO_3)_2 \cdot 6H_2O$), urea (H_2NCONH_2) and butylamine ($C_4H_{11}N$). First, $Zn(NO_3)_2 \cdot 6H_2O$ was added to the mixture of the MeOH–TEA solution with vigorous stirring. Then urea (or butylamine) was added to the mixed solution and heated by a hotplate at the same time. As temperature increased, the white precipitate appeared gradually. The white precipitation powders were thoroughly washed with deionized water and ultra-filtered through a 0.22 μm pore-size filter (Millipore Co., Bedford, MA). This procedure was repeated several times until a clear transmission electron microscopy (TEM) photograph of the precipitate was achieved.

In the present study, in order to produce spherical and fine grain-size ZnO powders, we controlled the nucleation and growth of the particles by means of adequate precipitant, heating rate, and the ratio of deionized water to methanol. The fabrication processes and results are shown in Fig. 1 and Table 1, respectively. Methanol and deionized water are found to give the best dispersion and solvent. TEA tends to make the ZnO particles more spherical. It is found that the heating hotplate gives a temperature gradient, and that the vaporization of mixed solution gives a concentration gradient. Both gradients can interfere with the ideal nucleation and growth.

The ZnO powder precipitated by urea will hereinafter be referred to as ZnO-I and that precipitated by butylamine as ZnO-II, while the varistor prepared by ZnO-I powders as varistor-I and by ZnO-II powders, varistor-II. The resultant ZnO-I and ZnO-II powders were calcined in an alumina crucible at 800 °C for 2 h. Then, the 97 mol ZnO and 0.5 mol ($Bi_2O_3 + 2Sb_2O_3 + MnO + CoO + Cr_2O_3$) were used as the original materials. They were mixed by ball-milling in alcohol for 24 h. The mixture was dried and calcined in air at 600 °C for 2 h and sieved through a 320-mesh screen to produce a starting powder. The starting powder was packed at a pressure of 350 kg/cm^2 into disks (diameter 10 mm and thickness 2 mm). The samples were sintered for 1 h at three different temperatures, 1150, 1200 and 1250 °C. The temperature was increased to those values at a rate of 600 °C/h; the cooling rate was 240 °C/h [19].

2.2. Measurements

The morphology of the ZnO powders was observed by a transmission electron microscope (H-7100, Hitachi, Tokyo, Japan). The decomposition temperature of the intermediate compound, and consequently the appropriate calcination temperature for the synthesized powders, can be obtained by a thermogravimetric analyzer (SSC5000, Seiko, Japan). The formation of the ZnO structure was identified by X-ray diffraction (XRD, D5000, Siemens, Germany). The microstructure of the ZnO varistor samples was examined by a scanning electron microscope (S2500, Hitachi, Japan).

The electrical properties were measured by means of a two-probe method in which silver conductive epoxy was applied to opposite faces of the sintered disks. The I–V characteristics were measured by using a programmable curve tracer (370A, Tektronix, Beaverton, OR) at 25 °C. The withstanding-surge capability was measured with a surge generator (801-plus, KeyTek Co., Burlington, MA) at 25 °C. Varistor current and voltage were monitored with an oscilloscope (7834, Tektro-

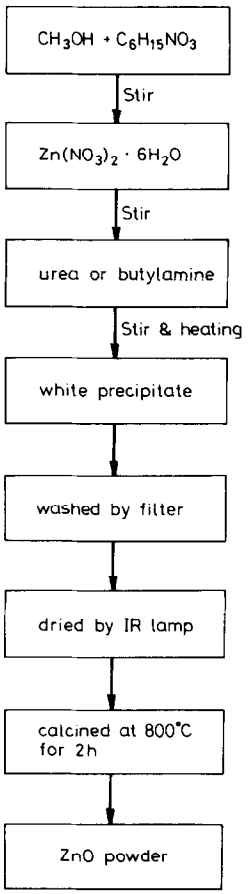

Fig. 1. Simplified flow diagram for the fabrication of the ZnO powder.

Table 1
Initial pH value (pH_i), final pH value (pH_f), precipitation time, precipitation temperature and precipitation rate for the ZnO powder prepared by the aqueous precipitation method

Precipitant	pH_i	pH_f	Time (min)	Temperature (°C)	Rate (%)
Urea	8.02	8.01	90	80	96.0
Butylamine	10.80	10.75	75	80	97.5

nix) with a 400 MHz bandwidth, digital storage and averaging capability.

3. Results and discussion

Fig. 2 shows the morphology of the ZnO-I and ZnO-II powders. The average particle sizes of the ZnO-I and ZnO-II powders are 0.8 and 0.6 μm, respectively. It is found that the ZnO-II powders are of uniform and well-shaped spherical particles, while the ZnO-I powders are less uniform in size. Fig. 3 shows the thermal evolution of the ZnO precipitates which was examined by thermogravimetry (TG) and differential thermal analysis (DTA) with a thermogravimetric analyzer. From the TG and DTA curves, the ZnO-I and ZnO-II precipitates demonstrate an obvious weight loss at a heating temperature below 440 and 450 °C, respectively. Therefore, better quality ZnO precipitates would be achieved with the calcination temperature above 500 °C. XRD results of the ZnO-I and ZnO-II powders showed that our products are pure crystalline ZnO.

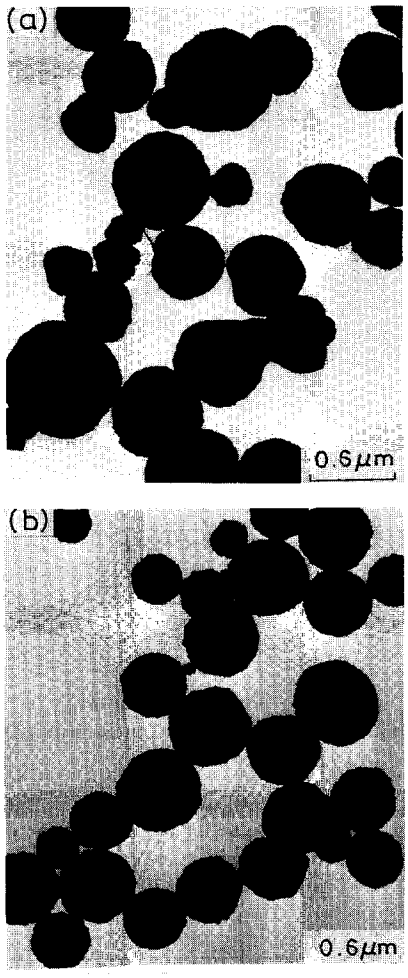

Fig. 2. Transmission electron micrographs of the ZnO powders: (a) ZnO-I; (b) ZnO-II.

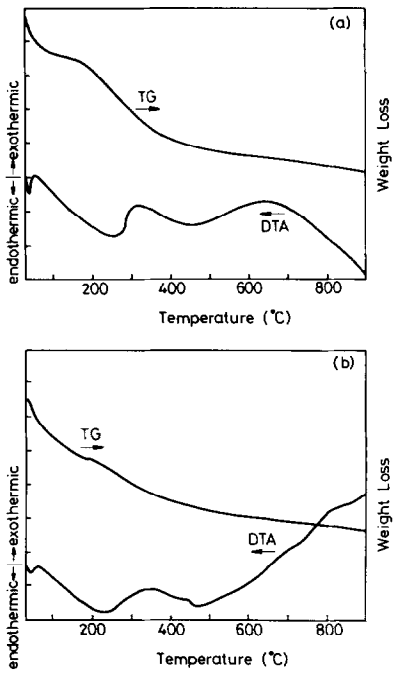

Fig. 3. TG and DTA curves of the ZnO powders: (a) ZnO-I; (b) ZnO-II.

The microstructure and XRD patterns of the ZnO varistor samples sintered at 1150 °C for 1 h are shown in Figs. 4 and 5, respectively. Their grain shapes are typical of recrystallized equilibrium structure and the main features of the microstructure are found to be the same as observed in several previous studies [20–23], i.e. along the multiple grain junctions of the ZnO grains, there lies a three-dimensional network of Bi_2O_3-rich intergranular phases, while, at the grain boundaries and within the ZnO grains, there occasionally exist spinel phases ($Zn_7Sb_2O_{12}$) in accordance with the composition of the ZnO varistors.

It is also found from Fig. 4 that the homogeneity of the microstructure of varistor-II is better than that of varistor-I. The average ZnO grain size of varistor-I is 9.91 ± 2.63 μm and that of varistor-II is 7.10 ± 1.25 μm. This is not surprising because the green powders for varistor-II are more uniform than that for varistor-I and it is known that large grains can easily grow by coalescence with small grains during sintering [24]. Therefore, the more homogeneous the ZnO powders, the more uniform grain growth occurs, and the more uniform microstructure of the ZnO varistors would be achieved.

Since the homogeneity of grain-size distribution plays a role in determining the electrical properties of the ZnO varistors [25–27], it is expected that varistor-II would have better electrical properties than those of varistor-I. We did find that the varistors prepared by ZnO-II powders had superior electrical properties to those made by ZnO-I powders under the conditions of the same composition and sintering process.

Fig. 6 shows the nonohmic I–V curves of varistor-I and varistor-II, both sintered at 1150 °C for 1 h. Their nonohmic properties were characterized by a nonohmic parameter α

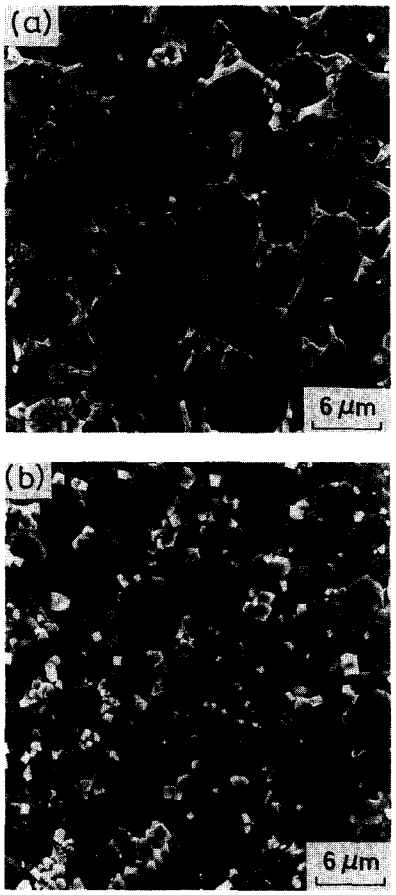

Fig. 4. Scanning electron micrographs of the microstructure of the ZnO varistor samples: (a) varistor-I; (b) varistor-II.

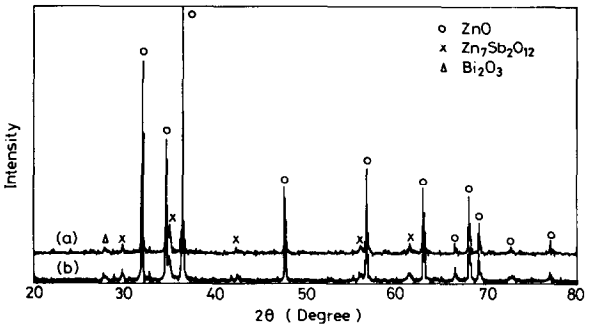

Fig. 5. XRD patterns of the ZnO varistor samples: (a) varistor-I; (b) varistor-II.

from the empirical formula $I = CV^{\alpha}$, where V stands for the voltage across the samples, I the current flowing through the samples and C a constant. The nonohmic parameters α were 75, 62 and 56 for varistor-II samples sintered at 1150, 1200 and 1250 °C, respectively; the nonohmic parameters α were 68, 51 and 30 for varistor-I samples sintered at 1150, 1200 and 1250 °C, respectively. The data provide evidence that the varistors made with ZnO-II powders show superior nonohmic electrical properties than those made with ZnO-I powders.

Besides the nonohmic parameter α, another important electrical property, i.e. the leakage current, was taken into consideration and it was found that varistor-II samples had smaller leakage current and the change of leakage current with sintering temperature was less sharp than that of varistor-I, although both the leakage current of varistor-II and varistor-I increased as the sintering temperature increased. The variation of leakage current, which was obtained under the breakdown voltage ($80\%V_{1mA/cm^2}$ d.c.), with various sintering temperatures for the samples of varistor-I and varistor-II is shown in Fig. 7.

The breakdown field of the two varistors was also investigated. It is shown in Fig. 7 that the breakdown field, which was measured under a current density $J = 1$ mA/cm^2, decreases as sintering temperature increases for both varistor-I and varistor-II. However, the breakdown field of varistor-II is larger than that of varistor-I, which is reasonable as the former has a smaller grain size than the latter.

We believe that the differences of the electrical properties, including nonohmic characteristic, leakage current and breakdown field, between varistor-I and varistor-II samples in our study result from the differences in homogeneity of the microstructures, since the homogeneity of the microstructure

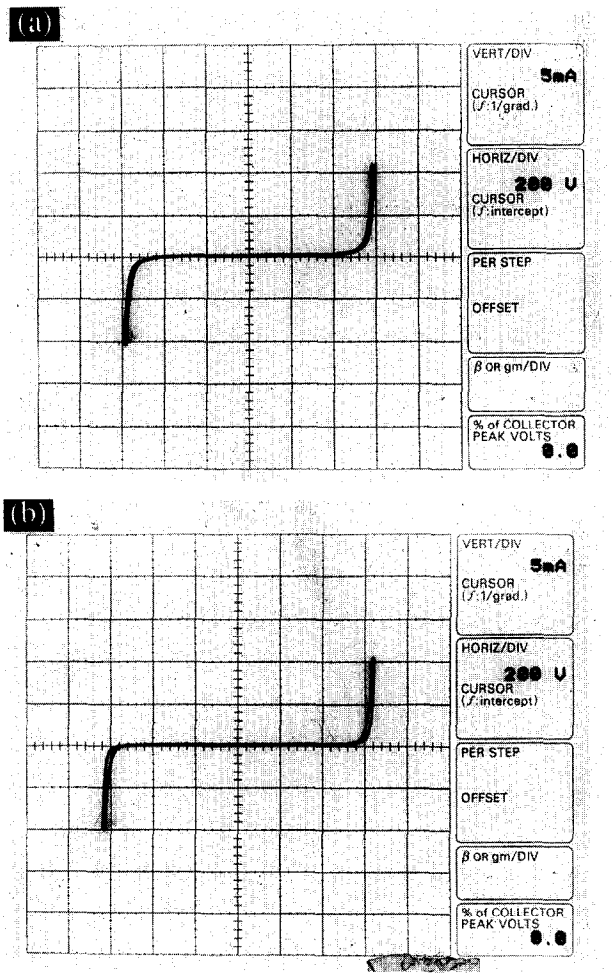

Fig. 6. Current–voltage tracers of the ZnO varistor samples: (a) varistor-I; (b) varistor-II. The applied voltage (200 V/div) is displayed on the horizontal axis and the current through the varistor on the vertical axis (5 mA/div).

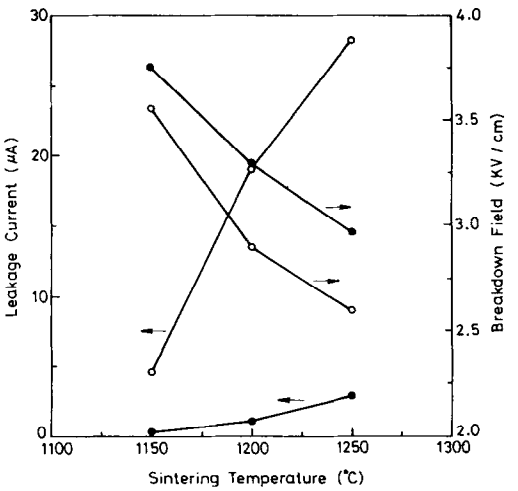

Fig. 7. Variations of the leakage current and the breakdown field with different sintering temperatures of the ZnO varistor samples: (○) varistor-I; (●) varistor-II.

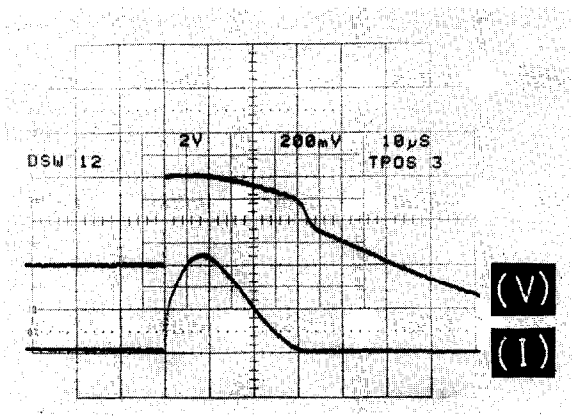

(a)

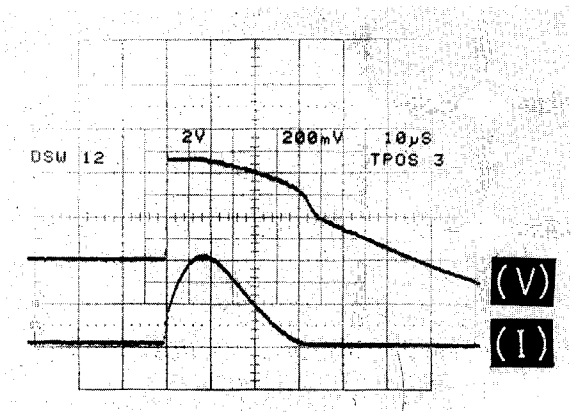

(b)

Fig. 8. Pulse response phenomena of the ZnO varistor samples: (a) varistor-I; (b) varistor-II (V: 400 V/div; I: 20 A/div; t: 10 μs/div).

is able to affect the grain-boundary properties which control the electrical properties of the ZnO varistors [28].

Pulse responses of varistor-I and varistor-II samples were both excellent as they were tested with a combination voltage–current surge wave. The voltage surge was 50 μs in duration with a rise time of 1.2 μs between 10% and 90% amplitude levels, while the surge current had a width of 20 μs and a rise time of 8 μs. As soon as the surge generator applied a voltage surge to the varistor samples, the surge current became available instantaneously. The observed surge responses are shown in Fig. 8.

Table 2
Pulse response parameters of varistor-I and varistor-II samples

Sintering temperature (°C)	Clamping voltage (V)	Peak current (A)	Dynamic resistance (Ω)
1150	1120 (I)	38 (I)	31 (I)
	1140 (II)	36 (II)	35 (II)
1200	900 (I)	40 (I)	27 (I)
	980 (II)	38 (II)	31 (II)
1250	800 (I)	44 (I)	20 (I)
	920 (I)	40 (II)	27 (II)

A summary of the measured parameters, derived from the surge response graphs in Fig. 8, is given in Table 2. From the table, we find that both the clamping voltage and the dynamic resistance of varistor-I and varistor-II samples decreased as the sintering temperature increased. The dynamic resistance, R_{dyn}, of the samples can be obtained from

$$\frac{V_{appl}}{R_{net}+R_{dyn}} = I_{peak} \quad (1)$$

where V_{appl} is the applied voltage, R_{net} the network resistance of the surge generator and I_{peak} the peak current which flows through the samples. However, varistor-II samples had higher clamping voltage, larger dynamic resistance and lower peak current than varistor-I samples. The clamping voltage decreased because the Schottky barrier height of the grain boundaries decreased with rising sintering temperature [29–31]. The smaller ZnO grain size of the varistor-II sample suggests a larger series resistance, in comparison with the varistor-I sample of the same thickness. The larger series resistance resulted in its lower peak current because the peak amplitude (3 kV) of the applied voltage surge fell at the upturn region.

4. Conclusions

The aqueous precipitation method is found to be a good way to produce ZnO powders, which, no matter whether they were precipitated by urea or butylamine, show pure crystalline ZnO from X-ray measurement. Between these two, the ZnO powders made from butylamine are more uniform, smaller, more well-shaped spherical particles than those made from urea. The average particle sizes are 0.6 and 0.8 μm for the powders made from butylamine and urea, respectively.

Although pulse responses of the varistor–butylamine and the varistor–urea are both excellent, the former displays superior electrical properties, including nonohmic characteristic

and leakage current, to the latter. The differences between their electrical properties are suggested to be due to the difference in homogeneity of the microstructures.

Acknowledgement

We gratefully acknowledge support from the National Science Council of Taiwan, ROC, under Project No. NSC 81-0404-E009-103.

References

[1] M. Matsuoka, *Jpn. J. Appl. Phys., 10* (1971) 736.
[2] L.M. Levinson and H.R. Philipp, *IEEE Trans. Parts Hybrids Packag., PHP-13* (1977) 338.
[3] M. Inada, *Jpn. J. Appl. Phys., 17* (1978) 673.
[4] P.R. Emtage, *J. Appl. Phys., 48* (1977) 4372.
[5] S. Fujitsu, H. Toyoda and H. Yanagida, *J. Am. Ceram. Soc., 70* (1987) C-71.
[6] M.A. Alim, *J. Am. Ceram. Soc., 72* (1989) 28.
[7] G. Hohenberger, G. Tomandl, R. Ebert and T. Taube, *J. Am. Ceram. Soc., 74* (1991) 2067.
[8] L.M. Levinson and H.R. Philipp, *Am. Ceram. Soc. Bull., 65* (1986) 639.
[9] J.D. Harnden, Jr., F.D. Martzloff, W.G. Morris and F.G. Golden, *Electronics, 10* (1972) 91.
[10] N. Amiji, Y. Tanno, H. Okuma and M. Kan, *Adv. Ceram. Mater., 1* (1986) 232.
[11] T. Asokan, G.N.K. Iyengar and G.R. Nagabhushana, *Ceram. Int., 14* (1988) 35.
[12] K. Eda, *J. Appl. Phys., 56* (1984) 2948.
[13] S.M. Haile, D.W. Johnson, Jr., G.H. Wiseman and H.K. Bowen, *J. Am. Ceram. Soc., 72* (1989) 2004.
[14] K. Kamata, H. Hosono, Y. Maeda and K. Miyokawa, *Chem. Lett.,* (1984) 2021.
[15] E. Sonder, T.C. Quinby and D.L. Kinser, *Am. Ceram. Soc. Bull., 64* (1985) 665.
[16] S. Hishita, Y. Yao and S.I. Shirasaki, *J. Am. Ceram. Soc., 72* (1989) 338.
[17] R.G. Dosch, B.A. Tuttle and R.A. Brooks, *J. Mater. Res., 1* (1986) 90.
[18] R.J. Lauf and W.D. Bond, *Am. Ceram. Soc. Bull., 63* (1984) 278.
[19] S.N. Bai and T.Y. Tseng, *Jpn. J. Appl. Phys., 31* (1992) 81.
[20] Y.S. Lee and T.Y. Tseng, *J. Am. Ceram. Soc., 75* (1992) 1636.
[21] M. Inada, *Jpn. J. Appl. Phys., 17* (1978) 1.
[22] H. Kanai, M. Imai and T. Takahashi, *J. Mater Sci., 20* (1985) 3957.
[23] E. Olsson, L.K.L. Falk, G.L. Dunlop and R. Österlund, *J. Mater. Sci., 20* (1985) 4091.
[24] W.D. Kingery, H.K. Bowen and D.R. Uhlmann, *Introduction to Ceramics,* Wiley, New York, 1976.
[25] P.R. Emtage, *J. Appl. Phys., 50* (1979) 6833.
[26] K. Eda, *IEEE Trans. Electr. Insul., 5* (1989) 28.
[27] D.F.K. Hennings, R. Hartung and P.J.L. Reijnen, *J. Am. Ceram. Soc., 73* (1990) 645.
[28] S.N. Bai and T.Y. Tseng, *J. Electron. Mater., 21* (1992) 1073.
[29] Y. Shim and J.F. Cordaro, *J. Am. Ceram. Soc., 71* (1988) 184.
[30] B. Bhushan, S.C. Kashyap and K.L. Chopra, *J. Appl. Phys., 53* (1981) 2932.
[31] J. Wong, *J. Appl. Phys., 51* (1980) 4453.